ISSN 1 746-7233, England, UK
World Journal of Modelling and Simulation
Vol. 11 (2015) No. 1, pp. 20-32

Dynamics of a cardiovascular model obtaining measurable pulsatile pressure output*

Aurelio A. de los Reyes V†

Institute of Mathematics, University of the Philippines Diliman C.P. Garcia St., U.P. Campus, Diliman, 1101 Quezon City, Philippines

(*Received November 25 2013, Accepted November 26 2014*)

Abstract. In this study, a lumped compartment cardiovascular model is developed to predict pulsatile pressures in the systemic and pulmonary circulation as well as in finger arteries. Essential compartments of the model include arterial and venous pulmonary, left and right ventricles, and arterial and venous systemic compartments. A pulsatile left ventricle is incorporated to be the source of pulse waves in the system. An aorta compartment is included to indicate pressure variations detected by baroreceptors acting as sensors in the cardiovascular system. Further, a finger artery is added as a typical site of pulsatile pressure measurements. In order to model the stiffness of heart muscles during exercise, a sigmoidal function dependent on heart rate is used to characterize the maximum left ventricular elastance. Numerical simulations of left-ventricular pressure and volume curves depicted its physiological dynamics. Moreover, the pulsatile cardiovascular model can be used to describe cardiovascular dynamics during rest and exercise conditions.

Keywords: mathematical cardiovascular model, pulsatile blood flow, left ventricle

1 Introduction

The cardiovascular system is a complex transport system providing various cells with the needed oxygen and other substrates for metabolism simultaneously removing carbon dioxide and other waste products of metabolism. Moreover, it transports hormones and enzymes which regulate cell functions. In general, its function is to maintain an appropriate environment in all tissue fluids of the body for optimal survival and function of the cells[21, 30, 33, 55, 65]. Since cardiovascular disease is the leading cause of deaths worldwide, efforts on experimental studies aim to examine its mechanisms and therapies. Mathematical modeling finds its way to analyze the cardiovascular system complementing experimental approach.

In the last decades, a large number of investigations regarding lumped parameter differential equation models have been developed to study dynamics and control of the cardiovascular system. Included are investigations on behavior of blood pressures in the peripheral and systemic compartments, cardiac output, ventricular elastance and contractility in the human circulatory system under various conditions. For instance, a mathematical cardiovascular model has been developed by Kappel and Peer to describe the response of the system to a constant workload[27]. It is based on the four-compartment model for the so-called mechanical part of the cardiovascular system by Grodins[19, 20]. Incorporated in the model are essential subsystems such as systemic and pulmonary circulation, left and right ventricles, baroreceptor loop, etc. Basic mechanisms such as Starling's law of the heart, the Bowditch effect, and autoregulation in peripheral regions are also included. The model satisfactory provided an overall description of the reaction of the cardiovascular system to a constant ergometric workload. Details on modeling issues, parameter estimation and simulations

* This work is supported by ASEA-UNINET Technologiestipendien Südostasien (Doktorat) scheme administered by the Austrian Academic Exchange Service (ÖAD) and the Austrian Grid 2 funded by BMWF-10.220/0002-II/10/2007.
† Corresponding author. *E-mail address*: adlreyes@math.upd.edu.ph.

with this model can be found in Batzel et al.[2]. Further studies extended the model to include the respiratory system[61] to describe the response of the cardiovascular-respiratory system under orthostatic stress situations induced by lower body negative pressure, head-up-tilt and postural changes[17, 25, 48, 66]; and to understand the underlying principles of congestive heart failure[3, 14]. These models typically predict blood pressure and flow in and between compartments representing various parts of the cardiovascular system. In recent years, cardiovascular system models increased its complexity to account more accurately the underlying physiological dynamics. For example, complex nonlinear models have been developed to describe the pulsatile pumping of the heart[7, 40, 44] and the blood flow and blood pressure regulation[15, 22, 40, 41, 62]. Furthermore, comprehensive cardiorespiratory models have been developed[16, 34]. A survey on cardiovascular-respiratory system regarding modeling, control issues and clinical problems arising from the control mechanisms can be found in Kappel and related work[4, 24].

The current study aims to develop a mathematical model capable of describing the response of the cardiovascular system during rest and exercise conditions. In particular, the model seek to predict pressures in the systemic and pulmonary circulation as well as pulsatile pressures in the finger arteries on different conditions such as rest and exercise phase. Driven by the principle of keeping the mathematical model as simple as possible and as complicated as necessary, a lumped parameter pulsatile cardiovascular system is developed. It incorporates essential subsystems such as arterial and venous pulmonary, left and right ventricles, and arterial and venous systemic compartments. An aorta compartment is included to indicate pressure variations detected by baroreceptors acting as sensors in the system. This is an important aspect in studying control regulatory mechanisms in the cardiovascular system[2, 3, 11, 17, 25, 27, 61] . Also, a finger artery compartment is added in which pulsatile pressure measurements can be obtained. In the current model, adjacent compartments are linked together by peripheral resistance. The cardiovascular model developed by Kappel and Peer[27] is extended to model pulsatility of blood flow using Olufsen's model of the left ventricle[40, 53]. Recently, the current pulsatile model has been investigated to describe the reaction of this system to a submaximal constant workload imposed on a person at a bicycle ergometer test after a period of rest[11]. Here, the focus is more on the physiological dynamics of left ventricular elastance and pressures during rest and exercise conditions. It has been observed that during exercise, the cardiovascular system responds with an elevated heart rate in order to increase blood flow in the stressed muscles and accordingly satisfy its increased oxygen demand. Taking into account the stiffness of heart muscles, maximum ventricular elastance is modelled as heart rate dependent. Hence, heart rate is considered to be one of the controlled parameters to simulate pressures at rest and during exercise. Numerical simulations also include the left ventricular volume and pressure during different stages in a heart cycle.

The paper is organized as follows: Section 2 provides details on the development of a pulsatile cardiovascular model. Numerical results, its interpretations and discussion are documented in Section 3. Conclusions and future work directions are presented in the last section.

2 A pulsatile cardiovascular model

In order to develop a lumped pulsatile cardiovascular model, two existing models are utilized: a nonpulsatile model adapted from Kappel and Peer[27] and a simplified pulsatile left heart developed by Olufsen et al.[53]. It is mathematically formulated in terms of an electric circuit analog, see Fig. 1. Blood pressure difference plays the role of voltage, blood flow plays the role of current, stressed volume plays the role of an electric charge, compliances of blood vessels play the role of capacitors, and resistors are the same in both analogies. Pressures, compliances and resistances are denoted by P, c and R, respectively. In the right ventricle, Q stands for the cardiac output and S for the contractility. The subscripts stand mainly for the name of compartments. That is, ap, vp, lv, sa, fa, as, vs, and rv correspond respectively to the arterial pulmonary, venous pulmonary, left ventricle, systemic aorta, finger arteries, arterial systemic, venous systemic and right ventricle compartments. Also, subscripts mv and av denote the mitral valve, respectively aortic valve. Moreover, sa_1 and sa_2 as subscripts for R (i.e., R_{sa_1} and R_{sa_2}) correspond to two different time-varying resistances connecting the systemic aorta to finger arteries and systemic aorta to arterial systemic compartment, respectively.

A pulsatile cardiovascular system is governed by the following differential equations:

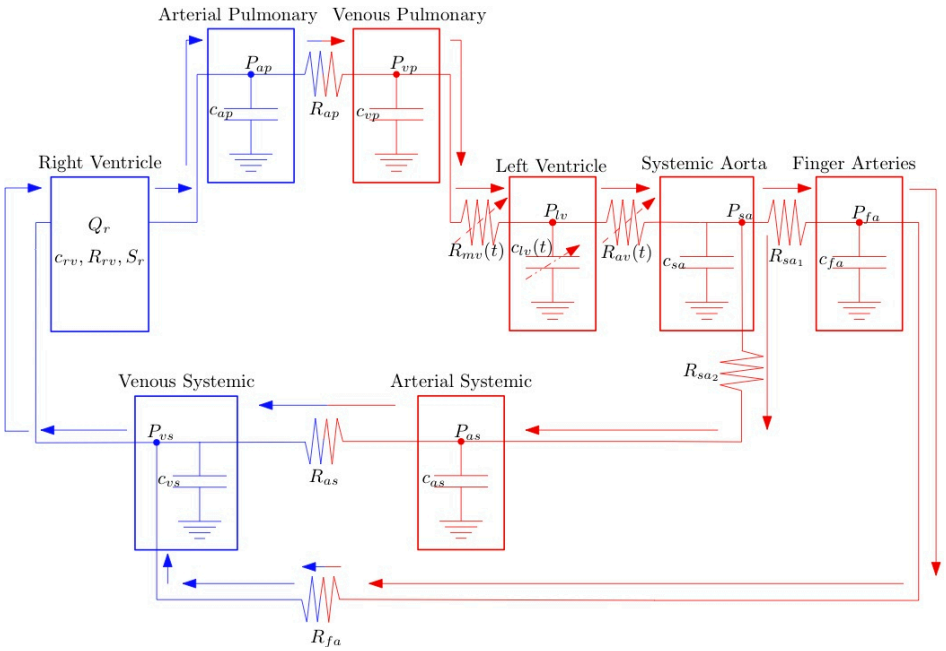

Fig. 1. Electric analog of the pulsatile model depicting the blood flow in the pulmonary and systemic circuits

$$
\begin{aligned}
\frac{dP_{sa}}{dt} &= \frac{1}{c_{sa}}\left(\frac{P_{\ell v}-P_{sa}}{R_{av}}-\frac{P_{sa}-P_{fa}}{R_{sa_1}}-\frac{P_{sa}-P_{as}}{R_{sa_2}}\right),\\
\frac{dP_{fa}}{dt} &= \frac{1}{c_{fa}}\left(\frac{P_{sa}-P_{fa}}{R_{sc_1}}-\frac{P_{fa}-P_{vs}}{R_{sp_f}}\right),\\
\frac{dP_{as}}{dt} &= \frac{1}{c_{as}}\left(\frac{P_{sa}-P_{as}}{R_{sc_2}}-\frac{P_{as}-P_{vs}}{R_{sp}}\right),\\
\frac{dP_{vs}}{dt} &= \frac{1}{c_{vs}}\left(\frac{P_{as}-P_{vs}}{R_{sp}}+\frac{P_{fa}-P_{vs}}{R_{sp_f}}-Q_{rv}\right),\\
\frac{dP_{ap}}{dt} &= \frac{1}{c_{ap}}\left(Q_{rv}-\frac{P_{ap}-P_{vp}}{R_{ap}}\right),\\
\frac{dP_{vp}}{dt} &= \frac{1}{c_{vp}}\left(\frac{P_{ap}-P_{vp}}{R_{ap}}-\frac{P_{vp}-P_{lv}}{R_{mv}}\right),\\
\frac{dP_{\ell v}}{dt} &= E_{\ell v}\left(\frac{\frac{dE_{\ell v}}{dt}P_{\ell v}}{{E_{\ell v}}^2}+\frac{P_{vp}-P_{\ell v}}{R_{mv}}-\frac{P_{\ell v}-P_{sa}}{R_{av}}\right),\\
\frac{dR_{sp}}{dt} &= \frac{1}{K}\left(A_{pesk}\left(\frac{P_{as}-P_{vs}}{R_{sp}}C_{a,O_2}-M_T\right)-(P_{as}-P_{vs})\right),\\
\frac{dS_{rv}}{dt} &= \sigma_{rv},\\
\frac{d\sigma_{rv}}{dt} &= -\alpha_{rv}S_{rv}-\gamma_{rv}\sigma_{rv}+\beta_{rv}H\ .
\end{aligned}
\tag{1}
$$

The following principle is applied for the first 7 differential equations in system (1): the total volume $V(t)$ in each compartment assumes a linear relation with the transmural pressure $P(t)$ as

$$V(t) = cP(t) + V_u, \tag{2}$$

where c represents compliance of the compartment and V_u denotes the unstressed volume. Moreover, blood flow follows a volume conservation and an analogue of Ohm's law.

The blood flow out of venous systemic compartment is the cardiac output $Q_{rv}(t)$ which is the blood flow into the arterial pulmonary given by

$$Q_{rv}(t) \;=\; HV_{str}(t), \tag{3}$$

where H is the heart rate and $V_{str}(t)$ is the stroke volume, that is, the blood volume ejected by one beat of the ventricle. Following Batzel et al.[2], the cardiac output of the right ventricle can be expressed as

$$Q_{rv}(t) \;=\; H\frac{c_{rv}P_{vp}(t)a_{rv}(H)f(S_{rv}(t),P_{ap}(t))}{a_{rv}(H)P_{ap}(t)+k_{rv}(H)f(S_{rv}(t),P_{ap}(t))}\,, \tag{4}$$

where

$$f(S_{rv}(t),P_{ap}(t)) \;=\; 0.5\,(S_r(t)+P_{ap}(t))-0.5\,((P_{ap}(t)-S_r(t))+0.01)^{1/2} \tag{5}$$

is a smooth function taking the minimum value between S_{rv} and P_{ap} at a specific time point t. This has been used in Timischl[61]. Also,

$$k_{rv}(H) \;=\; e^{-(c_{rv}R_{rv})^{-1}t_d(H)} \quad \text{and} \quad a_{rv}(H) \;=\; 1-k_{rv}(H)\,, \tag{6}$$

and

$$t_d(H) \;=\; \frac{1}{H^{1/2}}\left(\frac{1}{H^{1/2}}-\kappa\right), \tag{7}$$

where κ is in the range of 0.3-0.4 when time is measured in seconds and in the range of 0.0387-0.0516 when time is measured in minutes.

Opening and closing of the mitral and aortic valves are incorporated to model the left ventricle as a pump. We adapt the time-varying resistances as follows

$$\begin{aligned} R_{mv}(t) &= \min\left(R_{mv,open}+e^{(-10(P_{vp}(t)-P_{\ell v}(t)))},N\right),\\ R_{av}(t) &= \min\left(R_{av,open}+e^{(-10(P_{\ell v}(t)-P_{sa}(t)))},N\right), \end{aligned} \tag{8}$$

where $R_{mv}(t)$ and $R_{av}(t)$ are the time-varying mitral valve and aortic valve resistances, respectively, and N represents a large number. A small baseline resistance defines the "open" valve and a resistance which is several orders of magnitude larger defines the "closed" state. For instance, when $P_{\ell v}(t) < P_{vp}(t)$, the mitral valve opens and the blood enters the left ventricle. As $P_{\ell v}(t)$ increases and becomes greater than $P_{vp}(t)$, the resistance exponentially grows to a large value. The transition from open to closed valve is gradual. The value N is chosen to ensure that there is no flow when the valve is closed and remains there for the duration of the closed valve phase[15, 40, 41, 53]. We choose $N = 10,000$ in our numerical simulations.

According to Ottesen et al.[46], the relationship between the left ventricular pressure $P_{\ell v}$ and the stressed left ventricular volume $V_{\ell v}(t)$ is described by

$$P_{\ell v}(t) = E_{\ell v}(t)\,(V_{\ell v}(t)-V_d)\,, \tag{9}$$

where $E_{\ell v}(t)$ is the time-varying ventricular elastance and V_d (constant) is the ventricular volume at zero diastolic pressure.

In Pope et al.[53], the time-varying elastance function $E_{\ell v}(t)$ is given by

$$E_{\ell v}(t) = \begin{cases} E_m+\dfrac{E_M-E_m}{2}\left[1-\cos\left(\dfrac{\pi t}{T_M}\right)\right], & 0\le t\le T_M\\[2ex] E_m+\dfrac{E_M-E_m}{2}\left[\cos\left(\dfrac{\pi}{T_r}\,(t-T_M)\right)+1\right], & T_M\le t\le T_M+T_r\\[2ex] E_m, & T_M+T_r\le t<T\,. \end{cases} \tag{10}$$

This is a modification of the model developed by Heldt et al.[22] based on the previous detailed works by Danielsen and Ottesen[7, 44]. T_M denotes the time of peak elastance, and T_r is the time for the start of diastolic

relaxation, which are both functions of the length of cardiac cycle T. These parameters are set up as fractions where $T_{M,frac} = T_M/T$ and $T_{r,frac} = T_r/T$. Moreover, E_m and E_M are the minimum and maximum elastance values, respectively. The above elastance function (10) is sufficiently smooth. Its derivative can be easily computed as

$$\frac{dE_{\ell v}(t)}{dt} = \begin{cases} \dfrac{E_M - E_m}{2}\left[\dfrac{\pi}{T_M}\sin\left(\dfrac{\pi t}{T_M}\right)\right], & 0 \le t \le T_M \\ \dfrac{E_M - E_m}{2}\left[-\dfrac{\pi}{T_r}\sin\left(\dfrac{\pi}{T_r}(t - T_M)\right)\right], & T_M \le t \le T_M + T_r \\ 0, & T_M + T_r \le t < T\ . \end{cases} \tag{11}$$

The maximum elastance E_M can be interpreted as a measure of the contractile state of the ventricle[49, 59]. For normal resting heart, E_M can be a constant parameter. However, during exercise state, the contractility of heart muscles may increase as does the heart frequency. That is, heart rate and ventricular elastance are controlled in a concordant fashion, a mechanism referred to as the *Bowditch effect*[6]. As further modification, E_M is considered as a function dependent on heart rate H. Such function must be positive-valued, bounded and continuous. We choose the Gompertz function[18] for $E_M(H)$, a sigmoidal function given by

$$E_M(H) = a\exp(-b\exp(-cH)), \tag{12}$$

where a, b, c are positive constants. The constant a determines the upper bound of the function, b shifts the graph horizontally and c is the measure of steepness of the curve. The constants a, b and c were estimated obtaining $E_M = 2.4906[mmHg/mL]$ at $H = 70/60$ beats per second[46, 53].

Bazett's formula[5] is used for T_M as the time for systolic duration which is defined by

$$T_M = \frac{\kappa}{H^{1/2}}\ . \tag{13}$$

A submodel for the local metabolic regulation process in the tissue region is modeled under the assumption that arterial systemic resistance R_{as} depends on the venous oxygen concentration $C_{\mathrm{v,O_2}}$[51]:

$$R_{as} \ = \ A_{\mathrm{pesk}} C_{\mathrm{v,O_2}}, \tag{14}$$

where A_{pesk} is a positive constant. This relationship is based on the work of Huntsman on autoregulation [23] and was also used in other studies[3, 25, 27]. It describes the local constriction/relaxation mechanism acting on small vascular elements in response to local oxygen concentration $C_{\mathrm{v,O_2}}$ (some tissues also respond to $C_{\mathrm{v,CO_2}}$).

In order to model the cardiovascular system response to a constant ergometric workload W imposed on a test person on a bicycle ergometer, the following empirical formula for the metabolic rate is used:

$$M_{\mathrm{T}} \ = \ M_0 + \rho W\ , \tag{15}$$

where M_0 is the metabolic rate in the systemic tissue region corresponding to zero workload and ρ is a positive constant. As in Kappel and Peer's work[27], we have the relation:

$$M_{\mathrm{T}} \ = \ F_s\,(C_{\mathrm{a,O_2}} - C_{\mathrm{v,O_2}}) + M_b\ , \tag{16}$$

where F_s denotes the blood flow in the arterial systemic region and $C_{\mathrm{a,O_2}}$ denotes the concentration of O_2 in the arterial blood which is assumed to be constant. Moreover, for the biochemical energy flow, we assume that it is directly proportional on the rate of change of $C_{\mathrm{v,O_2}}$,

$$M_b \ = \ -K\frac{d}{dt}C_{\mathrm{a,O_2}}\ , \tag{17}$$

where K is a positive constant. Eq. (17) suggests that a positive amount of M_b is supplied whenever $C_{\mathrm{a,O_2}}$ is lowered. Differentiating Eq. (14) and combining it with Eq. (16), Eq. (17), and the flow equation to the

peripheral systemic region, we obtain the 8^{th} equation in system (1). In our model, we do not consider an autoregulation mechanism in finger arteries. This is due to the idea that in an ergometer bicycle test, the arms are held in a fixed position and hence, not directly involved in an exercise activity.

For the right ventricle, we consider the Bowditch effect of heart mechanism. The variations of the contractilities can be described by the following second order differential equation

$$\frac{d^2S_r}{dt^2} + \gamma_r \frac{dS_r}{dt} + \alpha_r S_r = \beta_r H, \tag{18}$$

where α_r, β_r and γ_r are constants. This set-up guarantees that the contractility S_r varies in the same direction as the heart rate H. Introducing the state variable $\sigma_r = \dfrac{S_r}{dt}$ and transforming (18) into systems of first order differential equations lead to the last two equations in system (1) [2, 27].

Further details in modeling development can be found in de los Reyes[10] and related works[9, 12].

3 Results and discussion

The parameters, its meaning and corresponding units used in the simulations can be found in Tab. 1. Most of the values are taken from the literature[2, 27] and some are estimated. Tab. 2 provides the controlled parameters which we vary to capture dynamics during rest and exercise simulations.

Table 1. Table of parameter values

Compliance	Meaning	Value	Unit
c_{sa}	Compliance in systemic aorta	1.75	mL/mmHg
c_{fa}	Compliance in finger arteries	0.05	mL/mmHg
c_{as}	Compliance in arterial systemic	3.25	mL/mmHg
c_{vs}	Compliance in venous systemic	850.95	mL/mmHg
c_{rv}	Compliance in relaxed right ventricle	44.131	mL/mmHg
c_{ap}	Compliance in arterial pulmonary	25.15	mL/mmHg
c_{vp}	Compliance in venous pulmonary	200.75	mL/mmHg
$c_{\ell v}$	Compliance in relaxed left ventricle	25	mL/mmHg
$R_{mv,open}$	Resistance when the mitral valve is open	0.0025	mmHg sec/mL
$R_{av,open}$	Resistance when the aortic valve is open	0.0025	mmHg sec/mL
R_{sc_1}	Resistance between systemic aorta and finger arteries	0.4745	mmHg sec/mL
R_{sc_2}	Resistance between systemic aorta and arterial systemic	0.25	mmHg sec/mL
R_{sp_f}	Resistance between finger and venous systemic compartment	9.75	mmHg sec/mL
R_{rv}	Inflow resistance of the right ventricle	0.002502	mmHg sec/mL
R_{pp}	Resistance in the peripheral region of the pulmonary circuit	0.1097	mmHg sec/mL
α_{rv}	Coefficient of S_{rv} in the differential equation for S_{rv}	0.003969	sec^{-2}
γ_{rv}	Coefficient of $\frac{dS_{rv}}{dt}$ in the differential equation for S_{rv}	0.021125	sec^{-1}
β_{rv}	Coefficient of H in the differential equation for S_{rv}	0.01841	mmHg/sec
a	Constant in the Gompertz function	3	mmHg/mL
b	Constant in the Gompertz function	10	1
c	Constant in the Gompertz function	3.415	sec^{-1}
E_m	Minimum elastance value of the left heart	0.029	mmHg/mL
$T_{r,frac}$	Quotient between T_r and T, i.e. $T_{r,frac} = \dfrac{T_r}{T}$	0.15	1
V_d	Unstressed blood volume in the left ventricle	10	mL
κ	Constant in the Bazett's formula	0.35	sec
$C_{\text{a,O}_2}$	O_2 concentration in arterial systemic blood	0.2	1
K	Constant in the formula for the biochemical energy flow	5465.9	mL
M_0	Metabolic rate in the systemic tissue region with zero workload	5.83	mL/sec
ρ	Coefficient of W in $M_{\text{T}} = M_0 + \rho W^{\text{exer}}$	0.183	mL/(sec Watt)

Table 2. Controlled parameters

State	Meaning	Value		Unit
		Rest	Exercise	
H	Heart rate	70/60	95/60	beat/sec
W	Workload	0	50	Watt
A_{pesk}	Peskin's constant	7.2276	12.25	mmHg sec/mL

In this model, the left ventricle is the source of pulse waves in the cardiovascular system. It is an important factor in describing pulsatility of blood flow. Let us first describe relevant features of the left ventricular pressure and volume during normal rest condition.

Starting at the relaxation phase, the pressure in the left ventricle, $P_{\ell v}$ drops to the level of the venous pressure, P_{vp}. Then, the mitral valve opens which is the start of the filling process. $P_{\ell v}$ continues to decrease in a short while and start to increase until it again reaches P_{vp}. Here, the filling process ends and the mitral valve closes. At this point, we can measure the end-diastolic left ventricular pressure. $P_{\ell v}$ continues to increase until it reaches the systemic aortic pressure, P_{sa}. The aortic valve opens and the ejection process starts. $P_{\ell v}$ continues to increase along with P_{sa} and after some time it decreases to the same level of P_{sa} in which the aortic valve closes. This time, we can measure the end-systolic left ventricular pressure which is the end of the ejection process. Then, $P_{\ell v}$ decreases to the level of P_{vp} and the cycle continues. To simulate the above scenario we first need to determine four important time points for a complete heart cycle, namely, the time when filling process starts, when it ends, when ejection process starts and when it ends. To find these time points, we incorporated in the *option* for the `odesolver` a function called ***'Events'*** (see Matlab for detatils). In this function, we specify the four instances we want to determine. Fig. 2 shows the dynamics of left ventricular (blue), venous (green) and aortic (red) pressures depicting the relevant points in a heart cycle. The simulation runs for 1500 seconds and the plots are taken from the last two full heart cycle.

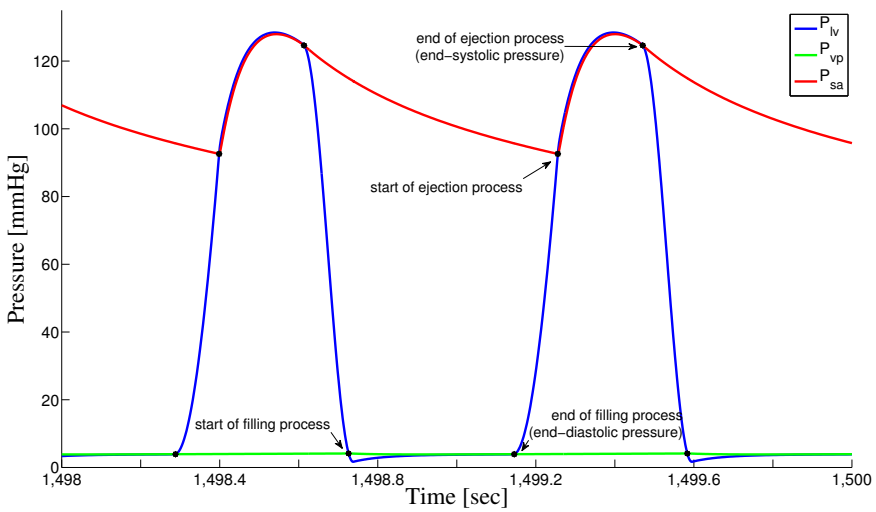

Fig. 2. Left ventricular (blue), venous (green) and aortic (red) pressures showing the time points for start and end of filling and ejection processes

Fig. 3 illustrates the computed left ventricular pressure (top panel) and volume (bottom panel) showing its behavior during phases of isovolumetric contraction and isovolumetric relaxation. Notice that during isovolumetric contraction, the pressure in the left ventricle is increasing while volume remains constant. During isovolumetric relaxation, pressure is decreasing while volume remains the same. The time points for these phases are numerically obtained using the *Events* specified earlier. The simulations are taken from one of the last complete pressure and volume cycles running for 1500 seconds.

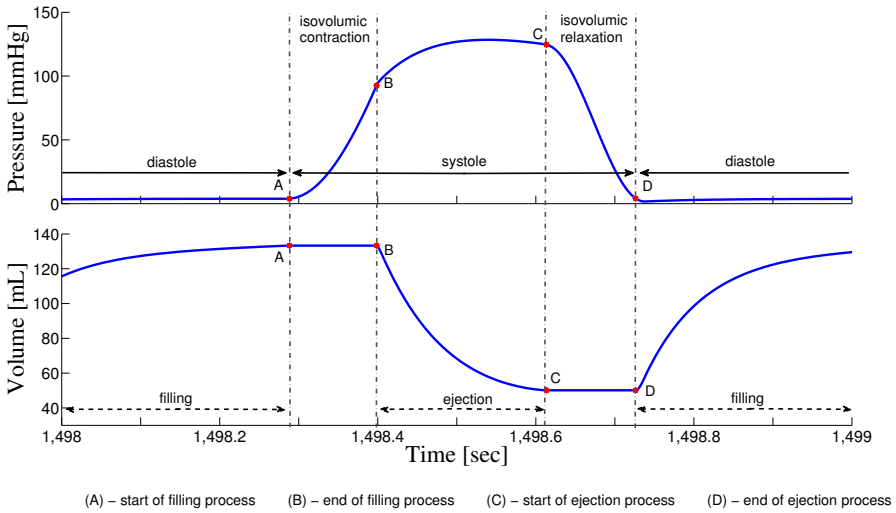

Fig. 3. Left ventricular pressure (top panel) and volume (bottom panel) depicting phases of isovolumetric contraction and isovolumetric relaxation

Let us summarize the left ventricular dynamics by providing the pressure-volume diagram, see Fig. 4. It depicts phases of a full heart cycle. At the end of ejection process, the pressure drops quickly while the volume remains constant. This is the phase of isovolumic relaxation (I). Then the mitral valve opens and the left ventricle is filled with blood, that is, phase of filling process (II). It is followed by a phase of isovolumetric contraction characterized by increasing left ventricular pressure while volume is constant. Then, the aortic valve opens and blood is propelled to the aorta with increasing pressure decreasing the volume in the left ventricle. The aortic valve closes at a point when the aortic pressure exceeds the left ventricular pressure. This completes the ejection phase (IV). Then the cycle continues. As in the previous plots, the red dots in the figure are obtained numerically using the specified events.

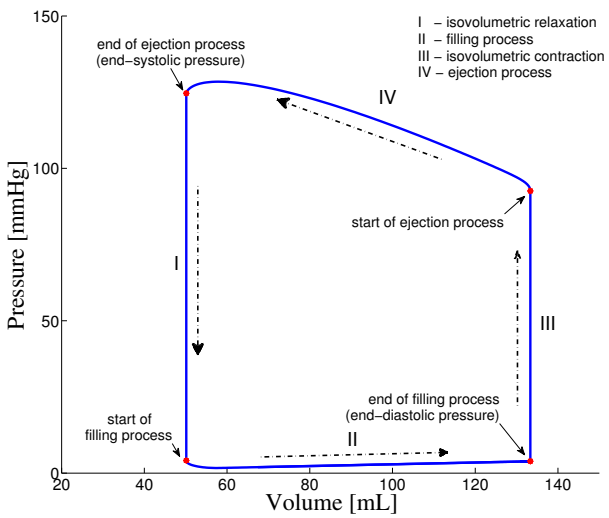

Fig. 4. Pressure-Volume diagram of the left ventricle showing the different phases in a complete heart cycle

Suppose at rest, heart rate is $H = 70/60$ beats per second and during exercise as in bicycle-ergometer test with minimal workload of 50 W, $H = 95/60$. Using Eqs. (10), (12), and (13), we obtain the elastance curves as depicted in Fig. 5. The blue and red dashed curves reflect the elastance at rest and exercise condition,

respectively. As can be observed, increasing heart rate leads to increased maximum elastance value, decreased in time for peak and smaller support of elastance curve.

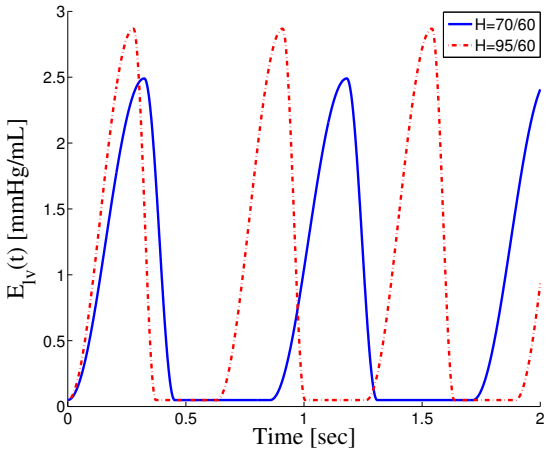

Fig. 5. Elastance function with varying heart rates

Now let us describe the reaction of the cardiovascular system under an imposed submaximal workload. As before, let us assume a bicycle-ergometer exercise with a workload of 50 W. Fig. 6 provides the time course of aortic (red) and left ventricular (blue) pressures during rest (dashed) and exercise (solid) conditions. As expected, pressures are increased during exercise. Phase shift and increased pulsatility are also observable. These are due to the modified time-varying elastance, which is dependent on heart rate as in previous section.

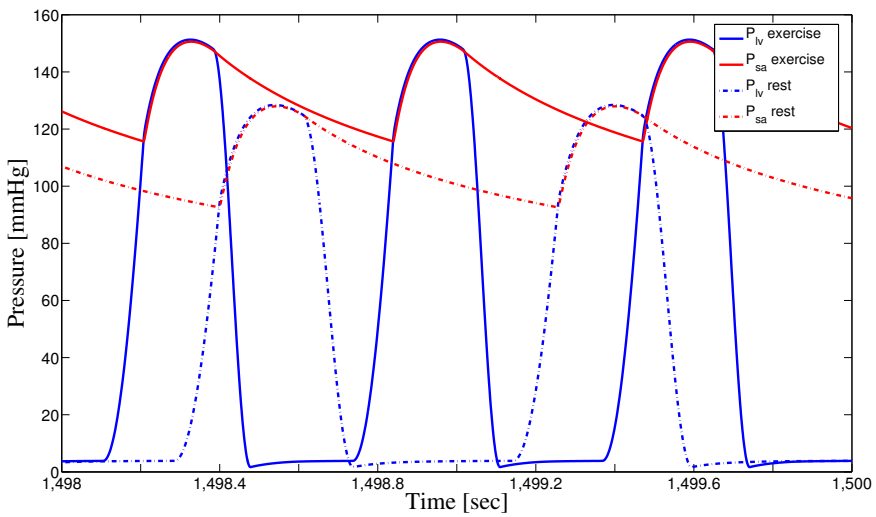

Fig. 6. Time course of the aortic and left ventricular pressures during rest and exercise phases

For this model, we can also compute the mean pressure given by

$$P_{\text{mean}} \;=\; P_{\text{dias}} + \frac{1}{3}\left(P_{\text{sys}} - P_{\text{dias}}\right), \tag{19}$$

where P_{dias} and P_{sys} are the end-diastolic and end-systolic pressures, respectively, and P_{mean} denotes the computed mean pressure[30]. End-systolic and end-diastolic pressures are specifed using the *Events* specified above. In Fig. 7, we have the finger arterial pressure during rest (dashed) and exercise (solid) conditions. The

red (dashed/solid) lines are the computed mean pressure using Eq. (19). Notice as well the increased pressure and pulsatility during exercise state.

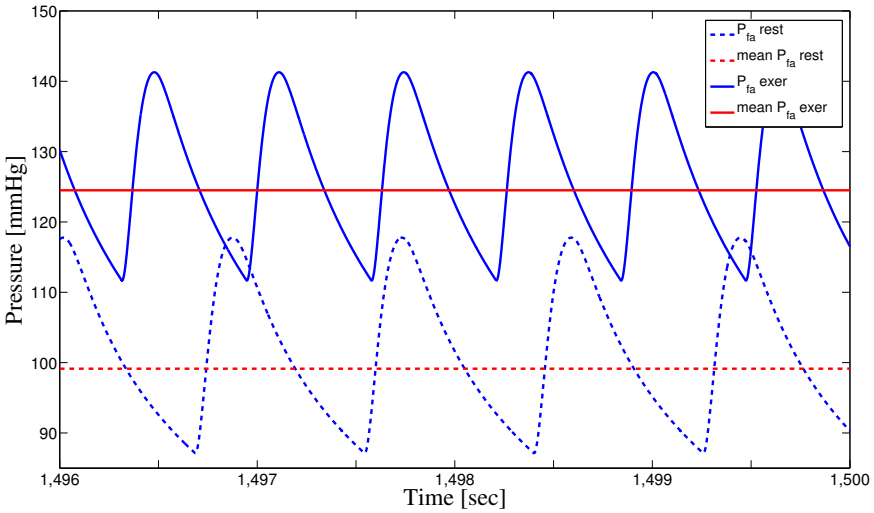

Fig. 7. Time course of finger arterial pressure during rest and exercise phases

4 Conclusion

A large number of mathematical cardiovascular models have been investigated from different perspectives depending on purposes and goals to be achieved. It vary from simple to complex and complicated models. In this paper, we presented a lumped compartment model, sufficiently simple to contain all essential subsystems such as arterial and venous pulmonary, left and right ventricles, and arterial and venous systemic compartments. However, it is complex enough to include heart rate dependent left ventricle elastance and capture pulsatile blood flow that can be measured in finger arteries. In this model, an aorta compartment is included to indicate pressure variations detected by baroreceptors which plays a role in describing regulation processes acted upon by baroreceptor loop. The latter is responsible for the increased heart rate and maximum elastance during exerise conditions and other stress-related activities imposed on the cardiovascular system.

An elaborate left ventricular dynamics is presented capturing its relevant physiological behaviour such as phases of heart cycle including isovolumetric contraction and relaxation. In pulsating pressures, timing for end of filling and end of ejection processes are numerically specified. This leads to determining end-diastolic and end-systolic pressures from which mean arterial pressure can be obtained. Another feature of the model is its capability of simulating exercise condition as in bicycle-ergometer by varying heart rate and other controlled parameters. An application of the current model include the design of feedback control described by the baroreceptor loop providing information on the transition dynamics of the cardiovascular system from rest to exercise phase[10, 11].

Patient-specific information can be obtained by parameter estimation via solving inverse problem and sensitivity analysis[1], given real-time data from performing bicycle ergometer test experiments. The current pulsatile model can be used to investigate transition dynamics of cardiovascular system under orthostatic stress. In particular, upper and lower parts of the arterial systemic and venous systemic compartments can be incorporated giving room to the rib and hips compartment in which orthostatic stress induced by lower body negative pressure can be studied. Furthermore, respiratory system and a brain compartment with the corresponding control regulations can be further included to have a more holistic global pulsatile circulatory model. Considering these regulatory mechanisms under several conditios, safer exercise protocols can be designed for individuals at risk especially for cardiac rehabilitation.

References

[1] H. Banks, A. Cintrón-Arias, F. Kappel. Parameter selection methods in inverse problem formulation. **in:** *Mathematical Modeling and Validation in Physiology*, Lecture Notes in Mathematics, Springer Berlin Heidelberg, 2013, 43–73.

[2] J. Batzel, F. Kappel, et al. *Cardiovascular and Respiratory Systems: Modeling, Analysis and Control*. SIAM, 2007, **34**.

[3] J. Batzel, F. Kappel, S. Timischl-Teschl. A cardiovascular-respiratory control system model including state delay with application to congestive heart failure in humans. *Journal of Mathematical Biology*, 2005, **50**(3): 293–335.

[4] J. Batzel, M. Bachar, et al. Merging mathematical and physiological knowledge: Dimensions and challenges. **in:** *Mathematical Modeling and Validation in Physiology*, Lecture Notes in Mathematics, Springer Berlin Heidelberg, 2013, 3–19.

[5] H. Bazett. An analysis of the time-relations of electrocardiograms. *Heart*, 1920, **7**: 353–370.

[6] H. Bowditch. Über die Eigenthüemlichkeiten der Reizbarkeit, welche die Muskelfasern des Herzens zeigen. *Verh. K Sachs Gen Wochenschr Leipzig Math Phys Cl*, 1871, **23**: 652–669.

[7] M. Danielsen, J. Ottesen. Describing the pumping heart as a pressure source. *Journal of Theoretical Biology*, 2001, **212**(1): 71–81.

[8] M. Danielsen, J. Ottesen. A dynamical approach to the baroreceptor regulation of the cardiovascular system. **in:** *Proceeding to the 5th International Symposium*, Symbiosis 97, 1997, 25–29.

[9] A. Reyes, F. Kappel. A mathematical cardiovascular model with pulsatile and non-pulsatile components. *Tech. Rep.*, University of Graz, SpezialForschungsBereich, 2010.

[10] A. Reyes. *A Mathematical Model for the Cardiovascular System with a Measurable Pulsatile Pressure Output*. Ph.D. Thesis, University of Graz, Institute for Mathematics and Scientific Computing, 2010.

[11] A. Reyes, E. Jung, F. Kappel. Stabilizing control for a pulsatile cardiovascular mathematical model. *Bulletin of Mathematical Biology*, 2014, **76**(6): 1306–1332.

[12] A.Reyes, F. Kappel. Modeling pulsatility in the human cardiovascular system. *Mathematica Balkanica*, 2010, **24**: 229–242.

[13] E. Doubek. Least energy regulation of the arterial system. *Bulletin of mathematical biology*, 1978, **40**(1): 79–93.

[14] L. Ellwein, S. Pope, et al. Patient-specific modeling of cardiovascular and respiratory dynamics during hypercapnia. *Mathematical Biosciences*, 2013, **241**(1): 56–74.

[15] L. Ellwein, H. Tran, et al. Sensitivity analysis and model assessment: Mathematical models for arterial blood flow and blood pressure. *Cardiovascular Engineering*, 2008, **8**: 94–108.

[16] H. Fan, M. Khoo. Pneuma-a comprehensive cardiorespiratory model. **in:** *Engineering in Medicine and Biology, 2002. 24th Annual Conference and the Annual Fall Meeting of the Biomedical Engineering Society EMBS/BMES Conference, 2002. Proceedings of the Second Joint*, 2002, **2**: 1533–1534.

[17] M. Fink, J. Batzel, F. Kappel. An optimal control approach to modeling the cardiovascular-respiratory system: An application to orthostatic stress. *Cardiovascular Engineering: An International Journal*, 2004, **4**(1): 27–38.

[18] B. Gompertz. On the nature of the function expressive of the law of human mortality, and on a new mode of determining the value of life contingencies. *Philosophical Transactions of the Royal Society London*, 1825, **115**: 513–583.

[19] F. Grodins. Integrative cardiovascular physiology: A mathematical synthesis of cardiac and blood vessel hemodynamics. *Quarterly Review of Biology*, 1959, **34**(2): 93–116.

[20] F. Grodins. *Control theory and Biological Systems*. New York London: Columbia University Press, 1963.

[21] A. Guyton, J. Hall. *Textbook of Medical Physiology*, Elsevier, 2006.

[22] T. Heldt, E. Shim, et al. Computational modeling of cardiovascular response to orthostatic stress. *Journal of Applied Physiology*, 2002, **92**(3): 1239–1254.

[23] L. Huntsman, A. Noordergraaf, E. Attinger. Metabolic autoregulation of blood flow in skeletal muscle: a model. **in:** *Cardiovascular System Dynamics*, MIT Press, Cambridge, 1978, 400–414.

[24] F. Kappel. Modeling the dynamics of the cardiovascular-respiratory system (CVRS) in humans, a survey. *Mathematical Modelling of Natural Phenomena*, 2012, **7**(05): 65–77.

[25] F. Kappel, M. Fink, J. Batzel. Aspects of control of the cardiovascular-respiratory system during orthostatic stress induced by lower body negative pressure. *Mathematical Biosciences*, 2007, **206**(2): 273–308.

[26] F. Kappel, S. Lafer, R. Peer. A model for the cardiovascular system under an ergometric workload. *Surveys on Mathematics for Industry*, 1997, **7**: 239–250.

[27] F. Kappel, R. Peer. A mathematical model for fundamental regulation processes in the cardiovascular system. *Journal of mathematical biology*, 1993, **31**(6): 611–631.

[28] T. Kenner. Physical and mathematical modeling in cardiovascular systems. **in:** *Clinical and Research Applications of Engineering Principles*, University Park Press, Baltimore, 1979, 41–109.

[29] T. Kenner, K. Pfeiffer. Studies on the optimal matching between heart and arterial system. **in:** *Cardiac Dynamics*, *Developments in Cardiovascular Medicine*, Springer Netherlands, 1980, **2**: 261–270.
[30] R. Klabunde. *Cardiovascular Physiology Concepts*, Lippincott Williams & Wilkins, 2011.
[31] H. Kwakernaak, R. Sivan. *Linear Optimal Control Systems*. New York London Sydney Toronto: Wiley-Interscience, 1972.
[32] S. Lafer. *Mathematical Modelling of the Baroreceptor Loop*. Ph.D. Thesis, University of Graz, Institute for Mathematics and Scientific Computing, 1996.
[33] R. Levick. *An Introduction to Cardiovascular Physiology*, 5th edn. CRC Press, 2009.
[34] K. Lu, J. Clark, et al. A human cardiopulmonary system model applied to the analysis of the valsalva maneuver. *American Journal of Physiology-Heart and Circulatory Physiology*, 2001, **281**(6): H2661–H2679.
[35] E. Noldus. Optimal control aspects of left ventricular ejection dynamics. *Journal of theoretical biology*, 1976, **63**(2): 275–309.
[36] A. Noordergraaf. *Hemodynamics in Biological Engineering*. McGraw-Hill, New York, 1969.
[37] A. Noordergraaf, J. Melbin. Introducing the pump equation. **in:** *Cardiovascular System Dynamics: Models and Measurements*, Plenum Press; New York, 1982, 19–35.
[38] M. Olufsen, A. Alston, et al. Modeling heart rate regulation part i: Sit-to-stand versus head-up tilt. *Cardiovascular Engineering*, 2008, **8**: 73–87.
[39] M. Olufsen, J. Ottesen. A practical approach to parameter estimation applied to model predicting heart rate regulation. *Journal of Mathematical Biology*, 2012, 1–30.
[40] M. Olufsen, J. Ottesen, et al. Blood pressure and blood flow variation during postural change from sitting to standing: model development and validation. *Journal of Applied Physiology*, 2005, **99**(4): 1523–1537.
[41] M. Olufsen, H. Tran, J. Ottesen. Modeling cerebral blood flow control during posture change from sitting to standing. *Cardiovascular Engineering*, 2004, **4**: 47–58.
[42] M. Olufsen, H. Tran, et al. Modeling baroreflex regulation of heart rate during orthostatic stress. *American Journal of Physiology-Regulatory, Integrative and Comparative Physiology*, 2006, **291**(5): R1355–R1368.
[43] K. Ono, T. Uozumi, et al. The optimal cardiovascular regulation of the arterial blood pressure. **in:** *Cardiovascular System Dynamics: Model and Measurements*, Plenum Press; New York, 1982, 119–139.
[44] J. Ottesen, M. Danielsen. Modeling ventricular contraction with heart rate changes. *Journal of Theoretical Biology*, 2003, **222**(3): 337–346.
[45] J. Ottesen, M. Olufsen. Functionality of the baroreceptor nerves in heart rate regulation. *Computer Methods and Programs in Biomedicine*, 2011, **101**(2): 208–219. Cardiopulmonary Modelling-Extended selected papers from the 7th IFAC Symposium on Modelling and Control in Biomedical Sysytems (MCBMS'09).
[46] J. Ottesen, M. Olufsen, J. Larsen. *Applied Mathematical Models in Human Physiology*. SIAM, Philadelphia, PA, 2004.
[47] J. Ottesen. Modelling of the baroreflex-feedback mechanism with time-delay. *Journal of mathematical biology*, 1997, **36**(1): 41–63.
[48] J. Ottesen, V. Novak, M. Olufsen. Development of patient specific cardiovascular models predicting dynamics in response to orthostatic stress challenges. **in:** *Mathematical Modeling and Validation in Physiology*, Lecture Notes in Mathematics, Springer Berlin Heidelberg, 2013, 177–213.
[49] J. Palladino, A. Noordergraafs. A paradigm for quantifying ventricular contraction. *Cellular & Molecular Biology Letters*, 2002, **7**(2): 331–335.
[50] J. Palladino, R. Zukus, et al. Left ventricular model parameters and cardiac rate variability. **in:** *Engineering in Medicine and Biology Society,EMBC, 2011 Annual International Conference of the IEEE*, 2011, 6817–6820.
[51] C. Peskin. *Mathematical Aspects of Physiology (Lectures in Applied Mathematics)*, American Mathematical Society, 1981, **19**.
[52] K. Pfeiffer, T. Kenner. On the optimal strategy of cardiac ejection. **in:** *Cardiovascular System Dynamics: Models and Measurements*, Plenum Press; New York, 1981, 133–136.
[53] S. Pope, L. Ellwein, et al. Estimation and identification of parameters in a lumped cerebrovascular model. *Mathematical Biosciences and Engineering*, 2009, **6**(1): 93–115.
[54] D. Regen, W. Howe, et al. Characteristics of single isovolumic left-ventricular pressure waves of dog hearts in situ. *Heart Vessels*, 1993, **8**(3): 136–148.
[55] R. Rhoades, G. Tanner. *Medical Physiology*, 2nd edn. Wolters Kluwer Health, 2003.
[56] V. Rideout. *Mathematical and Computer Modeling of Physiological Systems*. Prentice Hall, Englewood Cliffs, NJ, 1991.
[57] D. Russell. *Mathematics of Finite-Dimensional Control Systems-Theory and Design*. New York Basel: Marcel Dekker, 1979.
[58] K. Sughimoto, F. Liang, et al. Assessment of cardiovascular function by combining clinical data with a computational model of the cardiovascular system. *The Journal of Thoracic and Cardiovascular Surgery*, 2013, **145**(5):

1367–1372.

[59] K. Sunagawa, K. Sagawa. Models of ventricular contraction based on time-varying elastance. *Critical Reviews in Biomedical Engineering*, 1982, **7**(3): 193–228.

[60] G. Swan. *Applications of Optimal Control Theory in Biomedicine*. Marcel Dekker, 1984.

[61] S. Timischl. *A global model of the cardiovascular and respiratory system*. Ph.D. Thesis, University of Graz, Institute for Mathematics and Scientific Computing, 1998.

[62] M. Ursino. Interaction between carotid baroregulation and the pulsating heart: a mathematical model. *American Journal of Physiology-Heart and Circulatory Physiology*, 1998, **275**(5): 1733–1747.

[63] M. Ursino. A mathematical model of the carotid baroregulation in pulsating conditions. *IEEE Transactions on Biomedical Engineering*, 1999, **46**(4): 382–392.

[64] M. Ursino, A. Fiorenzi, E. Belardinelli. The role of pressure pulsatility in the carotid baroreflex control: A computer simulation study. *Computers in biology and medicine*, 1996, **26**(4): 297–314.

[65] N. Westerhof, N. Stergiopulos, M. Noble. *Snapshots of Hemodynamics*, *Basic Science for the Cardiologist*, Springer US, 2005, **18**.

[66] N. Williams, Ø. Wind-Willassen, et al. Patient-specific modelling of head-up tilt. *Mathematical Medicine and Biology*, 2014, **31**(4): 365–392.